Applied Catalysis A: General 482 (2014) 61–68

Contents lists available at ScienceDirect

Applied Catalysis A: General

journal homepage: www.elsevier.com/locate/apcata

Highly active Ga promoted Co-HMS-X catalyst towards styrene epoxidation reaction using molecular O_2

Sumbul Rahman[a], Chiranjit Santra[a], Rawesh Kumar[a], Jitendra Bahadur[b], Asima Sultana[c], Ralf Schweins[d], Debasis Sen[b], Sudip Maity[e], S. Mazumdar[b], Biswajit Chowdhury[a,*]

[a] Department of Applied Chemistry, Indian School of Mines, Dhanbad, India
[b] Solid State Physics Division, Bhabha Atomic Research Center (BARC), Mumbai, India
[c] National Institute of Advanced Industrial Science & Technology (AIST), Tsukuba, Japan
[d] Institut Laue-Langevin, Grenoble, France
[e] Central Institute of Mining and Fuel Research, Dhanbad, India

ARTICLE INFO

Article history:
Received 20 December 2013
Received in revised form 13 May 2014
Accepted 21 May 2014
Available online 29 May 2014

Keywords:
Mesoporous silica
Cobalt
Molecular oxygen
Epoxidation
Promoter
Gallium

ABSTRACT

Atom efficient synthesis of various value added products has been focused as an intense research area after Kyoto protocol. Styrene epoxidation is a challenging reaction as styrene epoxide is an important monomer for large number of polymers. It has been found that surface acidity and redox property of the catalyst has a major contribution to the catalytic activity for oxidation reaction. In this study Co-HMS-X catalyst was prepared and characterized by BET surface area and porosity measurement, SAXS, SANS, FESEM, HRTEM, UV–vis spectra, FTIR, ^{29}Si NMR, H_2-TPR and NH_3-TPD techniques. It is observed that 5 mol% Co-HMS-X showed highest catalytic activity for styrene epoxidation reaction using molecular O_2 as an oxidant. Interestingly it is found that among three different dopant (Al, Ga, Tl), the Ga promoted Co-HMS-X catalyst (Si:Co:Ga = 100:5:1.25) showed highest catalytic activity in terms of styrene conversion (100%) and styrene epoxide selectivity (68%). The unusual trend of Al, Ga and Tl towards the activity of Co-HMS-X (5 mol%) catalyst has been discussed from the results obtained in the H_2-TPR and NH_3-TPD study.

1. Introduction

In the 21st century, sustainable chemistry has been playing a key role in organic synthesis [1]. The atom efficient route for chemical reaction could motivate the chemist for replacing stoichiometric reactions using simple catalytic reactions. Among several reaction selective oxidations mainly epoxidation reactions deserve more attention as epoxides are important starting material for several value added products [2]. The direct epoxidation of ethylene using molecular oxygen over silver catalyst has opened a new horizon for the development of catalyst system which can demonstrate direct epoxidation of higher carbon number, e.g. propylene [3,4], 1-3 butadiene [5], cyclohexene, styrene as revealed in the literature [6,7].

Cobalt ions and their complexes are well known conventional homogeneous catalysts for the selective oxidation of alkenes using TBHP and O_2 as oxidizing agents [8]. Interaction of oxygen by cobalt complexes is venerable in biological system as well as organic synthesis. Uses of molecular oxygen as an oxidant with cobalt based catalysts are most desirable due to environment and economical consideration. Development of catalyst for styrene epoxidation using molecular oxygen as oxidant was started by cobalt salen complexes with need of sacrificial co-reductant such as isobutyraldehyde [9]. Though several heterogeneous cobalt catalysts have been reported for alkene epoxidation [9,10], however developing simple cobalt based catalyst without using co-reductant might be an interesting study from green chemistry perspective.

Till the discovery of MCM family mesoporous silica by Mobil researcher several types of mesoporous silica, e.g. SBA-15, TUD-1, KIT-6, FDU-16 have been developed [2,11] which could incorporate transition metal ions in its matrix demonstrating high activity for oxidation reaction [12,13]. Among several factor the control of acidic sites and redox property of the doped silica remained as a key factor for determining their catalytic activity [14]. It is often found that use of promoter has a significant contribution to improve the catalytic activity in the epoxidation of olefins. For the ethylene epoxidation calcium carbonate was used as a promoter for silver catalyst [15] whereas barium nitrate promoter was responsible

* Corresponding author. Tel.: +91 326 2235663; fax: +91 326 2296563.
E-mail address: biswajit_chem2003@yahoo.com (B. Chowdhury).

http://dx.doi.org/10.1016/j.apcata.2014.05.024
0926-860X/

for improving the catalytic activity of titanosilicate supported gold nanoparticle catalyst towards propylene epoxidation reaction [3,16]. The reason for the role of promoters varies in different cases but catalyst systems are much simpler as found in the system.

The newly developed two dimensional mesoporous silica HMS-X material has an advantage over conventional mesoporous silica because of having ordered hexagonal porous structure which can effectively help reactants to diffuse on the catalyst surface [17]. In the present study the three different loadings of Co-HMS-X (Si/Co = 20, 10 and 7) catalyst were prepared by sol–gel method and catalytic activities have been tested for styrene epoxidation reaction. It is found that fine tuning of acid–base and redox properties of ordered cobalt containing mesoporous silica catalyst might be helpful to get better activity towards direct epoxidation of styrene. Al, Ga and Tl (0.25 mol%) are used as promoters in cobalt containing mesoporous silica (Co-HMS-X 5 mol%) catalyst for styrene epoxidation reaction using molecular O_2. Ga promoted Co-HMS-X catalyst (Si:Co:Ga = 100:5:1.25) demonstrated 100% styrene conversion with 68% styrene oxide selectivity in the optimum reaction condition. The catalysts were characterized by several techniques, i.e. BET surface area and porosity measurements, SAXS, SANS, FESEM, HRTEM, UV–vis, FT-IR, ^{29}Si-NMR, H_2-TPR and NH_3-TPD techniques in order to elucidate the reason for high catalytic activity. The unusual trend of Al, Ga, and Tl towards the surface acidity of Co-HMS-X (5 mol%) catalyst resulting in different catalytic activity has been explained.

2. Experimental

2.1. Materials and catalyst preparation

Hexagonally ordered mesoporous Co-HMS-X was synthesized by using triblock copolymer as a template under acidic condition [17]. In a typical synthesis of 2D ordered mesoporous Co-HMS-X catalyst, Pluronic P123 (Aldrich) (4 g) was dissolved in 144 mL distilled water and 7.4 g 35% HCl (Merck) by continuous stirring. After stirring for 4 h a clear solution was obtained and then 4 g n-butanol (Merck) was added to this solution. The stirring was continued for 1 h. Tetraethyl orthosilicate (8.4 g) (TEOS, Acros) and aqueous solution of cobalt nitrate (0.81 g) (Aldrich) was added to this solution. The resulting gel composition of the mixture is P123:H_2O:HCl:n-butanol:TEOS:$Co(NO_3)_2{\cdot}6H_2O$ equal to 0.017:200:5.4:1.325:1:0.05–0.15 (molar ratio) and it was stirred for 24 h at room temperature. To prepare the metal nitrate promoted Co-HMS-X the gel composition is fixed as P123:H_2O:n-butanol:TEOS:$Co(NO_3)_2{\cdot}6H_2O$:$M(NO_3)_2$ equal to 0.017:200:5.4:1.325:1:0.05–0.15:0.0025 (molar ratio). Besides Al, Ga and Tl nitrate salts are also used for catalyst preparation. After stirring the mixture was taken in a closed polypropylene bottle and aged at 100 °C temperature for 24 h under static hydrothermal condition. After hydrothermal treatment the material was filtered in hot condition without washing and then dried at 100 °C for 12 h in air. Finally drying the material was calcined at 540 °C for 24 h. The material obtained after calcinations was labelled as Co-HMS-X and M-Co-HMS-X (M = Al, Ga, Tl).

2.2. Catalyst characterization

2.2.1. BET surface area and porosity measurement

The nitrogen adsorption–desorption isotherm of the samples were measured at liquid nitrogen temperature with a Quantachrome Nova-3200e at −196 °C. Pre-treatment of the samples were carried out at 300 °C for 3 h under high vacuum. The surface area was determined by Brunauer–Emmett–Teller (BET) equation. Pore size distributions were calculated using NLDFT (Non linear Density Functional Theory) model of cylindrical pore approximation.

2.2.2. Small angle X-ray scattering (SAXS)

Small-angle X-ray scattering (SAXS) measurements were performed using a laboratory based SAXS instrument with Cu K_α X-ray source. Variation of scattering intensity with wave vector transfer [$q = 4\pi \sin(\theta)/\lambda$] was measured for the powder samples.

2.2.3. Small angle neutron scattering (SANS)

Small-angle neutron scattering (SANS) experiments have been carried out at ILL, Grenoble, France using D11 instrument.

2.2.4. Field emission scanning electron microscope (FESEM)

Field emission scanning electron microscope (FESEM) was carried out by using Supra 55, Carl (Zeiss, Germany) microscope. Sample was supported on lacey carbon and then coated with platinum by plasma prior to measurement.

2.2.5. High resolution transmission electron microscope (HRTEM)

The HRTEM investigation was done on JEOL JEM 2100 microscope operated at 200 kV acceleration voltage using lacey carbon coated Cu grid of 300-mesh size.

2.2.6. Ultraviolet–visible spectroscope (UV–vis)

DRUV-Visible measurement was carried out by using Varian Cary 500 (Shimadzu) spectrophotometer. The spectra were recorded in the range of 190–500 nm wavelength.

2.2.7. Fourier transformation infrared spectroscopy (FT-IR)

The FT-IR measurements were carried out by using Perkin Elmer GX spectrophotometer. The spectra were recorded in the range of 400–4000 cm^{-1} using KBr pellet.

2.2.8. Magic-angle spinning nuclear magnetic resonance (MAS NMR)

^{29}Si MAS NMR was recorded at 500 MHz on Bruker advanced II-500 spectrometer equipped with a magic angle spin probe at room temperature.

2.2.9. Temperature programmed reduction (TPR)

TPR profiles of the samples are recorded with ChemiSorb 2720 (Micrometrics, USA) equipped with a TCD detector. The TPR profiles are obtained by reducing the catalyst samples by a gas mixture of 10% H_2 in Ar with a flow rate of 20 mL/min while the temperature is increased from ambient to 700 °C at a rate of 10 °C/min. Hydrogen consumptions in the profiles were evaluated by peak area of CuO TPR calibrations.

2.2.10. Temperature programmed desorption (TPD)

The acidity of the samples was measured by ammonia temperature-programmed desorption (NH_3-TPD) technique. A quadrapole mass spectrometer (BEL JAPAN) is used to detect desorbed NH_3, ca. 100 mg of the sample was outgassed at 500 °C for 1 h in a helium flow followed by ammonia adsorption at 100 °C for 1 h. Subsequently, the sample was flushed with helium for 30 min at 100 °C to remove physically adsorbed ammonia. Ammonia desorption was carried out by raising the temperature to 700 °C with a heating rate of 10 °C/min.

2.3. Styrene epoxidation reaction

Styrene epoxidation was carried out following the procedure reported in the literature [9]. In a typical procedure 10 mmol styrene (Acros), 10 mL DMF (Merck) and 0.2 mL internal standard (dodecane) were taken in a two neck 50 mL round bottle flask fitted

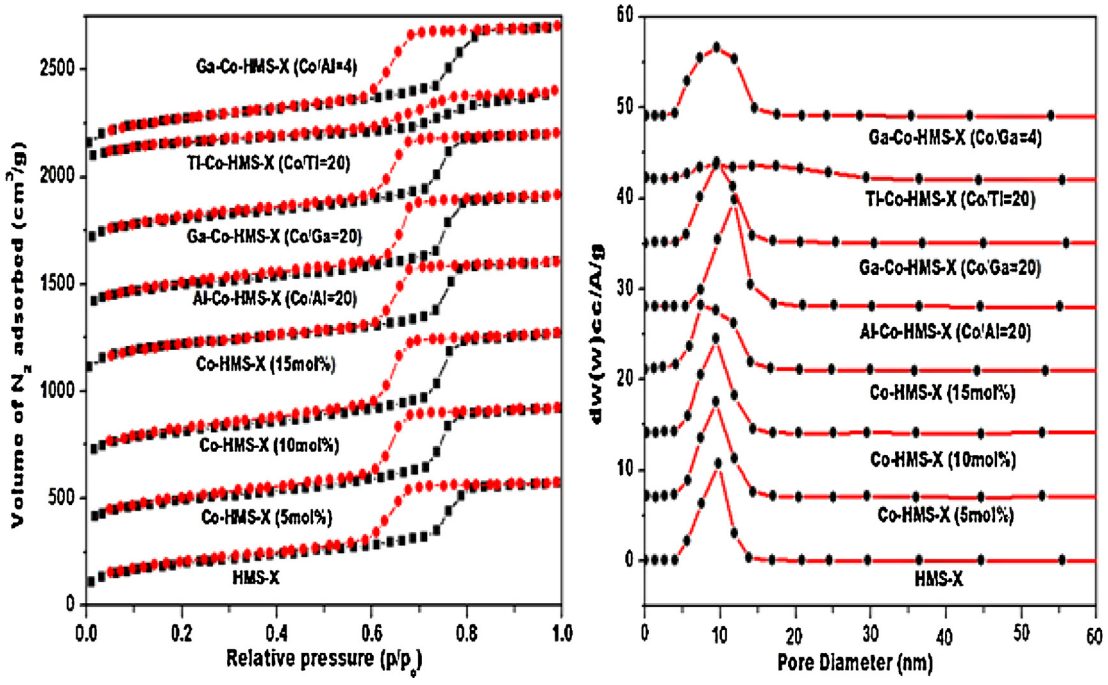

Fig. 1. Surface area and pore size of the catalyst.

with water condenser. Subsequently, 0.2 g catalyst was added to the reaction mixture followed by an appropriate oxygen flow (Aalborg mass flow controller) under constant stirring at 540 rpm using Tarson spinot digital magnetic stirrer. The reaction is carried for 4 h at 100 °C. The product analysis was done using a gas chromatograph (CIC-India) through SE-30 column.

3. Results and discussion

3.1. Textural characterization of the catalyst by BET surface area and porosity measurement

The BET surface area and porosity measurement results are depicted in Fig. 1. It is found that all materials has typical type IV adsorption/desorption isotherms with H1 hysteresis loop, which is characteristic of typical mesoporous materials. The sharp steps occurred at a relative partial pressure of 0.6–0.8, corresponding to the capillary condensation of N_2, which indicates the uniformity of the pores [2]. Pore structure parameters of HMS-X and Co-HMS-X calculated from the desorption branch are shown in Table S1 (supporting information). Compared with pure silica HMS-X, the introduction of cobalt made the surface area and pore volume significantly decrease. For Co-HMS-X, with increase of cobalt content, both the surface area and pore volume are gradually reduced. On increasing Co loading from 5 to 15 mol%, surface area of catalyst decreases from 674 to 621 m^2/g, this may be due to the sub-nanometer level cobalt species in the pores of silica as found in our recent study [17]. Interestingly it is observed that doping of Al, Ga and Tl has remarkably changed the surface area and pore size distribution. Doping of Tl destroyed the mesoporosity of Co-HMS-X material as revealed from adsorption isotherm and the surface area was quite low among the material (Table S1). A fine tuning of Co:Ga ratio could result in uniform pore size distribution, larger pore size and pore volume. The nature of interaction between PEO based templates and alkoxides controls the folding of templating agent which forms the ordered mesophase during synthesis [18]. May be higher basicity of Tl compared to others are responsible for collapse of mesophase in the present case.

3.2. Structural characterization of the catalyst by small angle X-ray scattering (SAXS) and small angle neutron scattering (SANS)

The SAXS patterns of various catalysts are shown in Fig. 2. A highly long range ordered mesoporous silica structure is evident from SAXS studies. Each sample exhibits an intense diffraction peak corresponding to the (1 0) plane at 0.64 nm^{-1}, typical characteristic of HMS material [19–21]. The intensity of the reflection corresponding to the (1 0), (1 1) and (2 0) planes decreases with the increase in cobalt loading as compared with the undoped siliceous HMS-X. This decrease in peak intensity upon higher Co loading compared to HMS-X analogue confirms change of the pore diameter in the mesoporous silica at higher cobalt loading. While comparing the results of Al, Ga and Tl, the ordered structure of HMS-X diminished

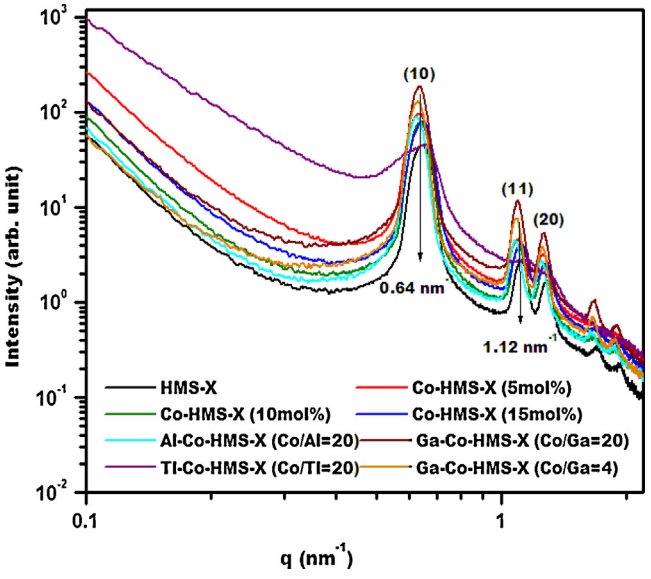

Fig. 2. The SAXS profiles for the catalyst.

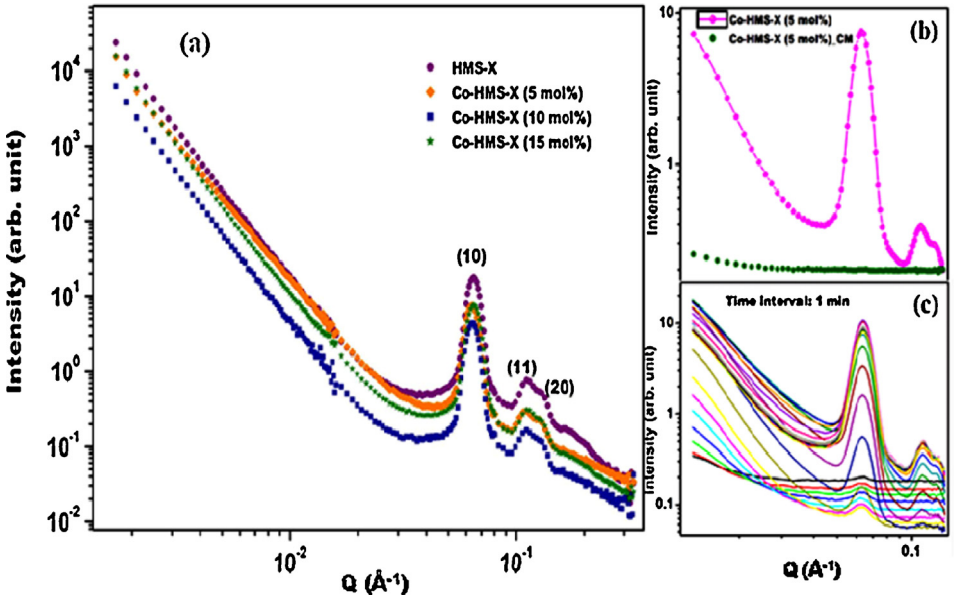

Fig. 3. (a) The SANS profiles for the catalyst. (b) The contrast match Co-HMS-X (5 mol%) and (c) the evolutions of scattering profiles for the contrast match Co-HMS-X (5 mol%) catalyst at 130 °C. "CM", contrast match; detector distance: 5 m.

after incorporation of Tl strengthening the results of BET surface area and porosity measurements.

Small angle neutron scattering experiment was found as a newly developed tool for characterizing the ordered mesoporous silica [22]. To know the accessibility of the pores in the HMS-X catalyst SANS characterization was carried out. Diffraction intensity analysis of small-angle scattering measurements of dry catalysts confirms the ordered mesopore structure. Fig. 3(a) shows the scattering curve over the 0.005–0.5 $Å^{-1}$ range due to the coherent scattering from the hexagonal array of primary mesopores results in the (1 0), (1 1) and (2 0) planes. Bragg diffraction peaks are 0.06, 0.104 and 0.13 $Å^{-1}$ respectively for the HMS-X and Co-HMS-X catalysts [23,24]. The intensities of the higher order (1 1) and (2 0) diffraction peaks show that the material has highly ordered structure. Contrast matching-small angle neutron scattering (CM-SANS) measurements have been carried out to probe the accessibility of the microspores using mixture of H_2O and D_2O. Typical survey scans are shown in Fig. 3(b) and (c). Here, diffraction intensity decreased below detection limit for the (1 0) peak at the contrast matching point and at the contrast match point, diffraction was eliminated completely, which implies that any micropores are larger than the water molecules are completely accessible [22,25]. Thus, all the pores in the present probed length scale are open in nature. Therefore, it can be said that agglomerated cobalt species are highly dispersed keeping the pores accessible to the reactant molecule.

3.3. Morphological study of the catalyst by FESEM and HRTEM characterization

From the FESEM image it is observed that the catalyst has worm-like morphology (Figs. S2 and S3, Supporting information) even at higher cobalt loading. Interestingly the morphology of HMS-X completely changed while Tl was doped in the Co-HMS-X which was unchanged in presence of dopant, e.g. Al and Ga in this present case. The HRTEM images (Fig. 4) of Co-HMS-X (Co/Si = 5/100) exhibits highly ordered hexagonal array of uniform channels. The ordered structure was not destroyed even at higher cobalt loading (Fig. S4, Supporting information). The XRD analysis could not detect any cobalt oxide species even at higher loading emphasizing the high dispersion of cobalt oxide species on the silica surface (Fig. S5, Supporting information). The EDS analyses (Fig. S6, Supporting information) confirm the presence of cobalt, silica and oxygen in Co-HMS-X catalyst.

3.4. Chemical characterization of the catalyst by UV–vis spectroscopy and FTIR spectroscopy

The UV–vis spectra of Co-HMS-X catalysts show two absorption peaks 529 nm and 590 nm (Fig. S7, Supporting information) which can be unambiguously assigned to the $^4A_2(F) \rightarrow {}^4T_1(P)$ transition of Co(II) ions in tetrahedral environments [26]. The blue colour of the catalyst is also a fingerprint of tetrahedral $Co(II)O_4$ sites. No such peak is observed in case of undoped HMS-X. The absorbance in the range of 500–700 nm is characteristic of Co(II) in an isolated state, the cobalt species in Co-HMS-X mainly exists in the state of single-site Co(II). However at higher loading there is appearance of absorption band around 250 nm region which is due to charge transfer between O^{2-} to Co^{2+} species [27]. The absence of clear peaks in the 500–700 nm region in Co-HMS-X (15 mol%) is observed on increasing the loading. This may be due to clustering of highly dispersed Co species in the silica matrix. The black spots in the HRTEM image and decrease in porosity for Co-HMS-X (15 mol%) (Fig. S4) strengthen the observation of UV–vis spectra.

The FTIR spectra of HMS-X and three differently loaded Co-HMS-X material are shown in Fig. S8 (Supporting information). The peaks at 1085 cm^{-1} and 1195 cm^{-1} are attributed to the asymmetric stretching vibration of framework Si—O—Si bridges. The peak at 817 cm^{-1} is attributed to Si—O—Si symmetric stretching. The gradual decrease of peak intensity at 817 cm^{-1} might be signifying the successive formation of Si—O—Co moiety. The peak at 960 cm^{-1} has been interpreted for stretching vibration of Si—OH and Si—O δ-groups. As found in literature the peak ascribed in the region 960 cm^{-1} can be considered as an evidence of the isomorphous substitution of Si by Co metal ions, i.e. as Si—O—Co connectivity [28]. This peak is also widely used to characterize the presence of transition metal atoms near the silica framework as the stretching Si—O vibration mode perturbed by the neighbouring metal ions. At higher loading this peak ramify, probably due to more diffusion

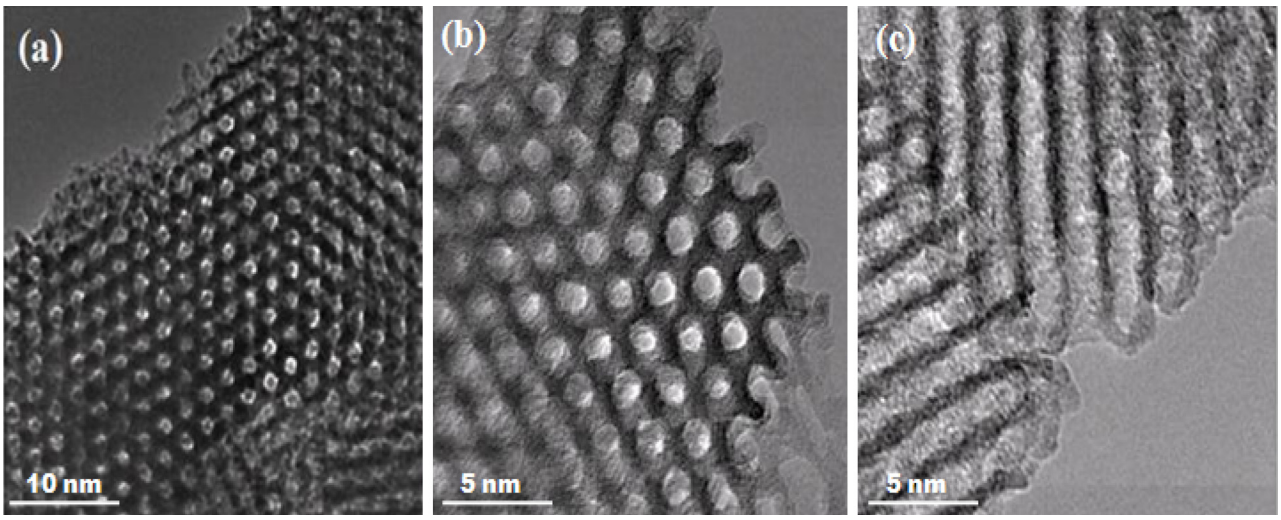

Fig. 4. HRTEM images of 5 mol% Co-HMS-X catalyst.

of cobalt oxide nanoparticles into the pores of silica matrix [17]. The bands appeared around 3500 cm^{-1} and 1633 cm^{-1} can be attributed to O—H and H—O—H respectively. As such there is no change in FTIR pattern for metal (Al, Ga and Tl) doped Co-HMS-X catalyst which is quite rational.

3.5. Characterization by ^{29}Si NMR spectroscopy

The ^{29}Si NMR spectra of Co-HMS-X depicted in Fig. 5, shows three different signals at −91, −101 and −110 ppm, similar to that obtained for doped mesoporous silica as reported in literature [17]. The first at around $\delta = -110$ ppm can be assigned to $(-O-)_4Si$ with no OH group attached to the silicon atom (Q^4). The second peak at $\delta = -101$ ppm is assigned to $(-O-)_3Si(OH)$ with one OH group (Q^3). The last peak at $\delta = -91$ ppm, is assigned to $(-O-)_2Si(OH)_2$ with two OH groups (Q^2). A close look on the ^{29}Si NMR of different cobalt loaded HMS-X reveals the decrease of Q^3 peak intensity at higher loading. It confirms that most of the cobalt species are not in the silica network. This kind of trend is also reported in literature [29].

3.6. Redox and acid–base characterization

The occurrence of multiple reduction peaks in TPR (*Temperature Programmed Reduction*) profile (Fig. 6) indicates the presence of a number of reducible cobalt species. The reduction of supported cobalt oxide was generally divided into two stages, a lower temperature region located between 254 and 487 °C could be assigned to the two step reduction of Co_3O_4 ($Co_3O_4 \rightarrow CoO \rightarrow Co$). The reduction behaviour of the high temperature region implies the degree of the interaction between the cobalt oxide and the support, forming Si—O—Co species which are difficult to be reduced [30]. The inset image in Fig. 6 shows that total hydrogen consumption is increased after addition of small amount of promoter (i.e. Al, Ga and Tl) in Co-HMS-X material. The promoter enhanced the reducibility of the catalysts which might be due to shift of reduction temperature at lower value compared with un-promoted Co-HMS-X catalyst.

NH_3-temperature programmed desorption (NH_3-TPD) was used to measure the total acidity and relative acid strength of the catalysts. Two-stage desorption of NH_3 over the promoted and unpromoted Co-HMS-X catalyst is observed from the TPD profiles as shown in Fig. 7. The first maxima in the temperature range of 200–340 °C can be assigned to weak chemisorptions of ammonia

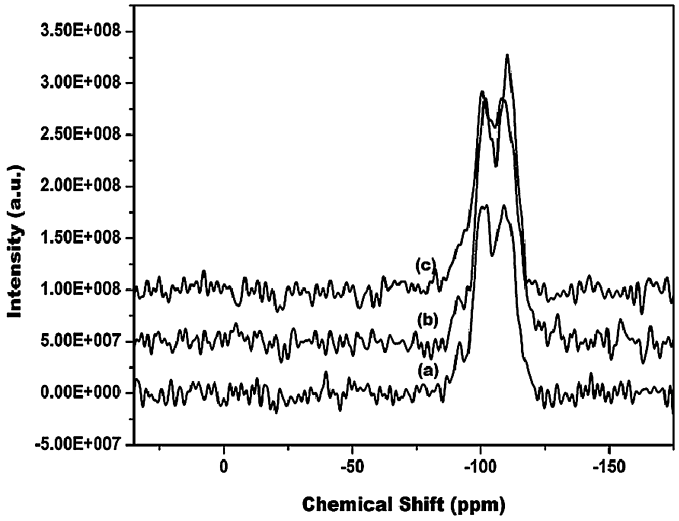

Fig. 5. ^{29}Si NMR spectra of the catalyst: (a) Co-HMS-X (5 mol%), (b) Co-HMS-X (10 mol%) and (c) Co-HMS-X (15 mol%).

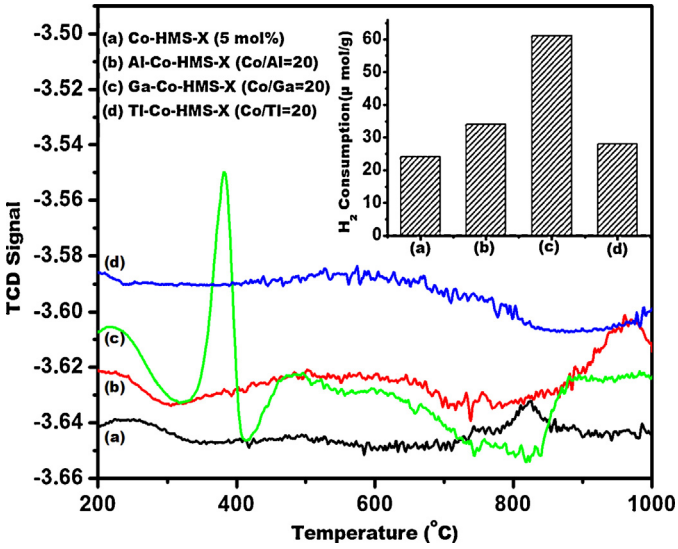

Fig. 6. H_2-TPR profile of the catalyst.

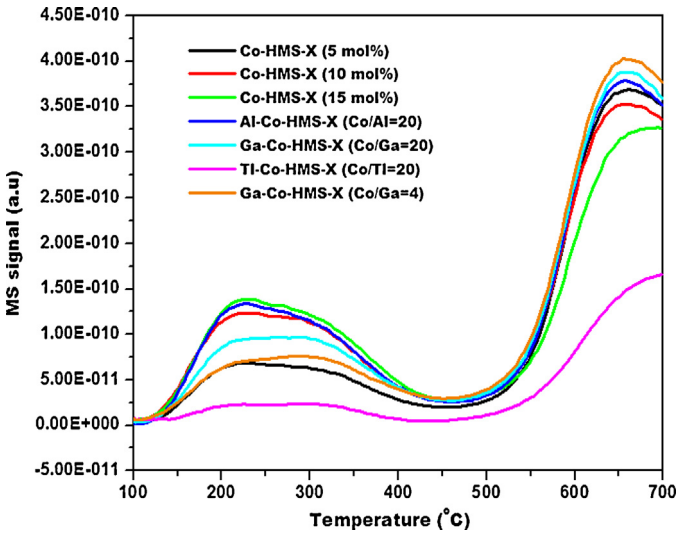

Fig. 7. NH_3-TPD profile of the catalyst.

inside the porous framework, possibly interacting with Lewis acidic site [14]. Desorption profile at ~660 °C might be due to chemisorption of ammonia on stronger acid sites [31]. A comparison of relative amount of acid sites shows that incorporation of Al in M-Co-HMS-X catalyst contribute to increase in acidity in the weak range, while the Ga incorporation in the strong range. The incorporation of Tl was found to decrease the acidity of Co-HMS-X catalyst in both the weak and strong range. Among the different percentage Ga loaded Co-HMS-X catalyst, the increase in Ga loading decreased the weak acidity and increased the strong acidity. The catalyst with Co/Ga ratio = 4 showed maximum number of acid sites in the strong acidity range. Increase of acidity in the strong range is expected to enhance the styrene epoxidation reaction as revealed in our previous studies [14].

3.7. Catalytic activity studies for styrene epoxidation reaction using molecular O_2

3.7.1. Effect of Co loading

Catalytic activities of 5, 10 and 15 mol% Co-HMS-X catalyst for styrene epoxidation reaction using molecular O_2 have been studied (Table S9, Supporting information). On increasing the cobalt loading from 5 to 15 mol%, a decrease in styrene conversion (i.e. 75.2–30.9%) and styrene oxide selectivity (i.e. 46.1–29.1%) is observed. It can be correlated from the surface area and porosity measurement data, where with increasing loading surface area and pore size were decreased. May be due to sub-nanometer cobalt oxide nanocluster species in the pores induce the lower accessibility for the active sites on the catalyst surface.

3.7.2. Effect of temperature

The influence of reaction temperature on the epoxidation of styrene with O_2 over Co-HMS-X have been studied (Table S10, Supporting information). The conversion of styrene increased sharply with the increasing of reaction temperature. For example, styrene conversion was 9.8% at 80 °C, quickly rose to 75.2% at 100 °C and 81.6% at 120 °C. But styrene conversion started to decrease with further increase of temperature. The rise in styrene conversion is decelerated to 72.5% at 140 °C. As reported in the literature [9] at temperature higher than 90 °C are probably rate determined by the diffusion of reactants to the active sites. It seems that an appropriate reaction temperature is favourable to the formation of epoxide for the reaction [2].

Table 1
Catalytic activity of the catalyst towards styrene epoxidation reaction.

Catalyst	Conversion (%)	Selectivity (%)	
		Styrene oxide	Benzaldehyde
Co-HMS-X (5 mol%)	90	59.8	40.2
Al-Co-HMS-X (Co/Al = 20)	100	35.3	64.7
Tl-Co-HMS-X (Co/Tl = 20)	75.7	30.1	69.9
Ga-Co-HMS-X (Co/Ga = 20)	100	61.6	38.4
Ga-Co-HMS-X (Co/Ga = 7)	100	60.8	39.2
Ga-Co-HMS-X (Co/Ga = 4)	100	67.5	32.5
Ga-Co-HMS-X (Co/Ga = 3)	100	59.9	40.1
Co-MCM-41 (0.78 wt.%) [8]	45	62.0	Others
Co-SBA-15 (20 wt.%) [2]	94	66.0	Others
Ga-TUD-1 (4 mol%) [14]	27	45.0	55.0
La-KIT-6 (0.04 wt.%) [33]	28	17.0	Others
Co-ZSM-5 (4 mol%) [34]	67	79.0	Others

Reaction conditions: solvent = DMF (20 mL); reactant = styrene (10 mmol); catalyst = 0.2 g; temperature = 120 °C; O_2 flow = 15 mL/min; time = 4 h.

3.7.3. Effect of O_2 flow rate

The influence of flow rate of O_2 on the epoxidation of styrene over Co-HMS-X at 120 °C has also been carried out (Table S11, Supporting information). The styrene conversion was 45.6% when flow rate was 5 mL/min, and then slowly increased to 90% with the rise of flow rate of O_2 to 15 mL/min. The styrene conversion is decreased when the flow rate of O_2 was higher than 15 mL/min which may be due to over oxidation of the substrate as reported in the literature [32].

3.7.4. Effect of solvent

The effect of solvent was studied in the optimum reaction temperature and oxygen flow which is also interesting (Table S12, Supporting information). There are several studies on the coordination of DMF or DMA to cobalt (II) complexes, and such coordination may affect the ability of O_2 to bind the cobalt complexes and their redox potential [9]. Although a certain styrene conversion was obtained in dimethyl sulfoxide (DMSO) and cyclohexanone, the epoxide selectivity was low, and the main product was benzaldehyde. So, it can be concluded that DMF is the best solvent for styrene oxidation reaction of cobalt based catalytic system [10].

3.7.5. Optimum condition

As discussed above by varying different conditions over 5 mol% Co-HMS-X catalyst, it is found that high oxygen flow rate, i.e. 15 mL/min, reaction temperature 120 °C, solvent DMF and 4 h time on stream are the optimum parameters to get best catalytic activity for this reaction (90% styrene conversion and 59.8% styrene oxide selectivity) as shown in Table 1.

3.7.6. Effect of different promoters

To improve the catalytic activity, the three different promoters Al, Ga and Tl are added to Co-HMS-X catalyst (5 mol%). Group III A metals are well known for their acidity where the acidity decreases in the order Al > Ga > Tl. Addition of promoter showed significant impact on styrene conversion and selectivity. The styrene conversion leads to 100% when Al and Ga are added as promoters but in case of Tl conversion decreases to 75.7%. The selectivity of epoxide followed up the trend of the styrene conversion; it reached to 61.5% in case of Ga and least in case of Tl. Again changing the Co/Ga ratio from 20 to 4, increase in styrene oxide selectivity has been observed, i.e. styrene oxide selectivity increases from 61.5% to 68% (Table 1), which is quite satisfactory with the literature report. After addition of promoter the change in catalytic activity of Co-HMS-X can be correlated with the H_2-TPR and NH_3-TPD results. The H_2-TPR study shows that among the three promoters (Al, Ga and Tl), Ga-Co-HMS-X (Si:Co:Ga = 100:5:0.25) has the highest H_2

Table 2
Catalytic activity of the catalyst during recycling and substrate variation towards epoxidation reaction.

Substrate	Catalyst	Conversion (%)	Selectivity (%)	
			Oxide[d]	Aldehyde[e]
Styrene	Co-HMS-X (5 mol%)	90.0	59.8	40.2
Styrene[a]	Co-HMS-X (5 mol%)	90.0	45.1	54.9
Styrene[b]	Co-HMS-X (5 mol%)	81.7	32.9	67.1
Styrene[c]	Co-HMS-X (5 mol%)	80.1	30.1	69.9
Cyclooctene	Co-HMS-X (5 mol%)	–	–	–
Cyclooctene	Ga-Co-HMS-X (Co/Ga = 20)	17	60.8	39.2
Cyclooctene	Ga-Co-HMS-X (Co/Ga = 4)	13.4	100	–
Stilbene	Ga-Co-HMS-X (Co/Ga = 20)	15	67.5	32.5

Reaction conditions: solvent = DMF (20 mL); reactant = styrene 10 mmol; catalyst = 0.2 g; temperature = 120 °C; O_2 flow = 15 mL/min; time = 4 h. 'a', 1st recycle; 'b', 2nd recycle; 'c', 3rd recycle.
[d] Corresponding oxide.
[e] Corresponding aldehyde.

consumption as well as NH_3-TPD profile indicates the presence of strong acidic sites into the catalyst surface. Lewis acid sites have an impact on metal–support interaction, perhaps influencing the cobalt reducibility. Thus, Ga-Co-HMS-X exhibits high reducibility in nature hence possesses high oxidizing property in comparison to the Al-Co-HMS-X and Tl-Co-HMS-X. A higher temperature desorption of ammonia is related to stronger acid sites. Among the Ga-Co-HMS-X, Co/Ga = 4 have the highest strengths of acid sites followed by Co/Ga = 20 > 7 > 3.

3.7.7. Catalytic regeneration and substrate variation

The catalyst recyclability is one of the important parameter to commercialize the catalyst. Catalytic activity of the catalysts almost unaffected up to three cycles as presented in Table 2. The marginal decrease observed in conversion may be due to the loss of catalyst during filtration and drying. A sharp decrease in selectivity of styrene oxide, probably due to formation of Co(II) → Co_3O_4 species led to increase in the formation of benzaldehyde. In addition, the Ga-Co-HMS-X (Co/Ga = 4) catalyst induced several epoxidation reaction of different substrate, e.g. cyclooctene, stilbene to the corresponding epoxide (Table 2).

3.7.8. Proposed reaction mechanism

It is interesting to note that in co-doped (M = Ga) catalyst, Co/Ga = 4 is needed to get 100% conversion and improved styrene oxide selectivity up to 68%. Based on the catalytic activity and literature survey a proposed mechanism for epoxidation of styrene with molecular oxygen at DMF solvent system over Co^{2+} catalyst has been depicted in Fig. 8 [10,35]. However the role of co-doped metal on styrene epoxidation reaction needs to be explained. The ionic radius of Co^{2+} and Ga^{3+} are more comparable (Co^{2+} = 65 pm, Ga^{3+} = 62 pm) rather than Al^{3+} (53 pm) or Tl^{3+} (150 pm). In case of gallium, it might be possible that Co^{2+} ion can be replaced by Ga^{3+} and hold into an interstitial site (like Frenkel defect). This causes defects as well as co-ordinatively unsaturated interstitial cobalt sites. The resultant cobalt complex [DMF-LCo(II)] was coordinated to molecular oxygen to form a cobalt superoxo complex DMF-LCo(III)OO•, which led to oxidative addition with styrene to give

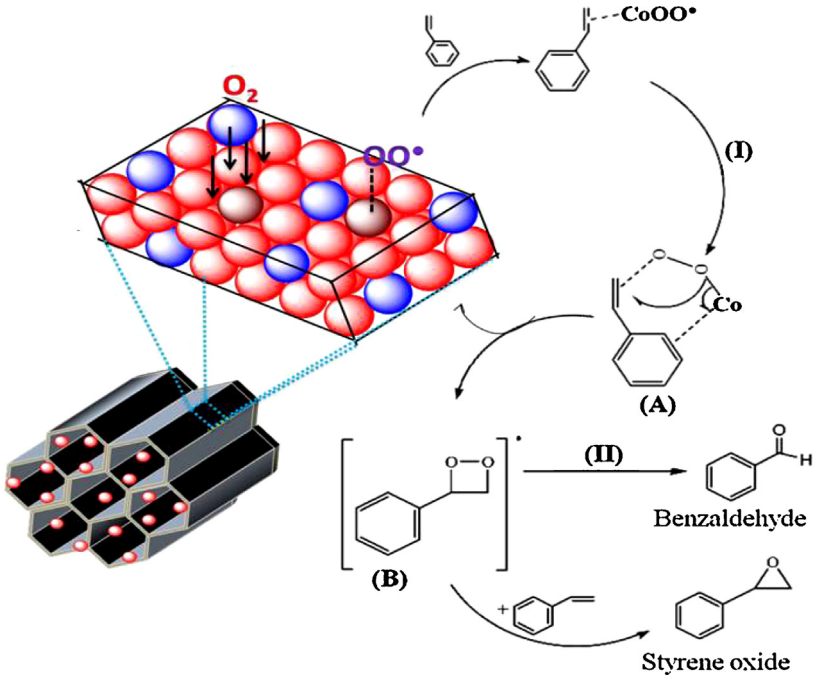

Fig. 8. Proposed reaction mechanism.

the styrene epoxide. Then due to migratory insertion, (path I) complex (A) was formed. This complex collapsed to the cyclic peroxide radical (B). The intermediate (B) underwent thermal decomposition to benzaldehyde or react with another styrene molecule to generate styrene oxide.

4. Conclusions

Co-HMS-X catalyst of different loading is synthesized by sol–gel method in which 5 mol% loading is found as optimum. Small angle X-ray scattering and small-angle neutron scattering results revealed that catalysts were mesoporous in nature as well as hexagonal pore structure. The HRTEM images of Co-HMS-X (5 mol%) shows presence of well-shaped uniform mesoporous surface. UV–vis results confirms that tetrahedral cobalt (II) was highly dispersed inside the HMS-X mesopores. It is the key factor for the epoxidation of styrene by molecular oxygen. ^{29}Si NMR result indicated the presence of three different types of silica species and Si—O—Co linkage, confirming the Co incorporation into Si framework. Both H_2-TPR and NH_3-TPD results revealed that Ga-Co catalyst is more reducible and acidity increases increasing Ga loading. Thus, the catalytic activity primarily depends on the acidity of the catalyst which in turn strongly depends on the gallium content in the sample. Interestingly, 100% conversion efficiency was found in case of Ga-Co-HMS-X (Co/Ga = 4) with 68% selectivity for styrene oxide.

Acknowledgments

SR and CS would like to acknowledge UGC, Govt. of India for research fellowship. BC would like to acknowledge UGC, Govt of India for funding in the research project [Project No. F.39-802/2010 (SR)]. RK acknowledge ISM for providing senior research fellowships.

Appendix A. Supplementary data

Supplementary data associated with this article can be found, in the online version, at http://dx.doi.org/10.1016/j.apcata.2014.05.024.

References

[1] H. Over, R. Schomäcker, ACS Catal. 3 (2013) 1034–1046.
[2] H. Cui, Y. Zhang, Z. Qiu, L. Zhao, Y. Zhu, Appl. Catal. B: Environ. 101 (2010) 45–53.
[3] B. Chowdhury, J.J. Bravo-Suárez, M. Date, S. Tsubota, M. Haruta, Angew. Chem. Int. Ed. 45 (2006) 412–415.
[4] J. Huang, T. Akita, J. Faye, T. Fujitani, T. Takei, M. Haruta, Angew. Chem. Int. Ed. 48 (2009) 7862–7866.
[5] P.L. Mills, J.F. Nicole, Ind. Eng. Chem. Res. 44 (2005) 6453–6465.
[6] S.K. Maiti, S. Dinda, M. Nandi, A. Bhaumik, R.G. Bhattacharyya, J. Mol. Catal. A: Chem. 287 (2008) 135–141.
[7] R.J. Chimentão, F. Medina, J.L.G. Fierro, J.E. Sueiras, Y. Cesteros, P. Salagre, J. Mol. Catal. A: Chem. 258 (2006) 346–354.
[8] B. Tyagi, B. Shaik, H.C. Bajaj, Appl. Catal. A: Gen. 383 (2010) 161–168.
[9] Q. Tang, Q. Zhang, H. Wu, Y. Wang, J. Catal. 230 (2005) 384–397.
[10] J. Sebastian, K.M. Jinka, R.V. Jasra, J. Catal. 244 (2006) 208–218.
[11] F. Jiao, H. Frei, Energy Environ. Sci. 3 (2010) 1018–1027.
[12] S.L. Jain, B.S. Rana, B. Singh, A.K. Sinha, A. Bhaumik, M. Nandi, B. Sain, Green Chem. 12 (2010) 374–377.
[13] A. Modak, M. Nandi, A. Bhaumik, Catal. Today 198 (2012) 45–51.
[14] S. Mandal, A. Sinha Mahapatra, B. Rakesh, R. Kumar, A. Panda, B. Chowdhury, Catal. Commun. 12 (2011) 734–738.
[15] B. Chowdhury, K.K. Bando, J.J. Bravo-Suarez, S. Tsubota, M. Haruta, J. Mol. Catal. A: Chem. 359 (2012) 21–27.
[16] G. Jenzer, T. Mallat, M. Maciejewski, F. Eigenmann, A. Baiker, Appl. Catal. A: Gen. 208 (2001) 125–133.
[17] S. Mandal, C. Santra, R. Kumar, M. Pramanik, S. Rahman, A. Bhaumik, S. Maity, D. Sen, B. Chowdhury, RSC Adv. 4 (2014) 845–854.
[18] G.J.A.A. Soler-Illia, C. Sanchez, New J. Chem. 24 (2000) 493–499.
[19] X.L. Yang, W.L. Dai, H. Chen, J.H. Xu, Y. Cao, H. Li, K. Fan, Appl. Catal. A: Gen. 283 (2005) 1–8.
[20] P.A. Robles-Dutenhefner, K.A. da Silva Rocha, E.M.B. Sousa, E.V. Gusevskaya, J. Catal. 265 (2009) 72–79.
[21] D. Sen, S. Mazumder, J.S. Melo, S. Arshad Khan, S.F. Bhattyacharya, D. Souza, Langmuir 25 (2009) 6690–6695.
[22] G.A. Zickler, S. Jähnert, W. Wagermaier, S.S. Funari, G.H. Findenegg, O. Paris, Phys. Rev. B 73 (2007) 184109.
[23] R.A. Pollock, B.R. Walsh, J. Fry, I.T. Ghampson, Y.B. Melnichenko, H. Kaiser, R. Pynn, W.J. DeSisto, M.C. Wheeler, B.G. Frederick, Chem. Mater. 23 (2011) 3828–3840.
[24] R.A. Pollock, G.Y. Gor, B.R. Walsh, J. Fry, I.T. Ghampson, Y.B. Melnichenko, H. Kaiser, W.J. DeSisto, M.C. Wheeler, B.G. Frederick, J. Phys. Chem. C 116 (2012) 22802–22814.
[25] J. Bahadur, D. Sen, S. Mazumder, S. Bhattacharya, H. Frielinghaus, G. Goerigk, Langmuir 27 (2011) 8404–8414.
[26] H. Ma, J. Xu, C. Chen, Q. Zhang, J. Ning, H. Miao, L. Zhou, X. Li, Catal. Lett. 113 (2007) 104–108.
[27] S. Farhadi, J. Safabakhsh, P. Zaringhadam, J. Nano Chem. 3 (2013) 69.
[28] T. Tsoncheva, L. Ivanova, J. Rosenholm, M. Linden, Appl. Catal. B: Environ. 89 (2009) 365–374.
[29] P. Bhangea, D.S. Bhangea, S. Pradhana, V. Ramaswamy, Appl. Catal. A: Gen. 400 (2011) 176–184.
[30] D. Song, J. Li, J. Mol. Catal. A: Chem. 247 (2006) 206–212.
[31] R. Ghosh, X. Shen, J.C. Villegas, Y. Ding, K. Malinger, S.L. Suib, J. Phys. Chem. B 110 (2006) 7592–7599.
[32] D. Jiang, T. Mallat, D.M. Meier, A. Urakawa, A. Baiker, J. Catal. 270 (2010) 26–33.
[33] Z. Wangcheng, G. Yanglong, W. Yanqin, G. Ynn, L. Guanzhong, J. Rare Earths 28 (2010) 369–375.
[34] G. Xu, Q.H. Xia, X.H. Lu, Q. Zhang, H.J. Zhan, J. Mol. Catal. A: Chem. 266 (2007) 180–187.
[35] H. Cui, Y. Zhang, L. Zhao, Y.Z. Cui, Y. Zhang, L. Zhao, Y. Zhu, Catal. Commun. 12 (2011) 417–420.